SUPPLEMENTARY EXPERIMENTAL PROCEDURES

RNA Analysis

RNA isolation (RNAeasy, Qiagen) and cDNA synthesis (Supercript choice system, Invitrogen) were performed according to the manufacturer's instructions. cDNA synthesis for analyses aiming to detect *Pax4* transcripts was performed using a mixture of eight *Pax4*-derived (and β-actin-derived) antisense oligonucleotides instead of the provided oligo-dT primers (Figure S6B).

Quantitative RT–PCR were carried out using the QuantiTect SYBR Green RT-PCR Kit (Qiagen) and validated primers (Qiagen) according to the manufacturer's instructions. The PCR reactions and detection were performed on a Mastercycler® ep realplex cycler using GAPDH and HPRT1 as internal controls for normalization purposes.

Lentiviral vector construction to specifically target *Ngn3*-expressing cells

A 5566-bp long fragment of the *Ngn3* promoter spanning from position -5286 to +280 relative to transcription start site was amplified by PCR from a genomic lambda clone containing the mouse *Ngn3* locus using the high fidelity Phusion DNA polymerase (FINNZYMES) with the following primers: pNgn3 Fw = 5' CACCAAGCTTTGTGTGGAAGGAAATGTC and pNgn3 Rv = CGCGCGCCCCTCATCCACCCTTTG. The resulting PCR product was cloned into the pENTR/D-Topo plasmid (Invitrogen) and the insert sequenced to rule out PCR-mediated mutations. The resulting plasmid was used to perform LR Clonase II (Invitrogen) *in vitro* recombination in order to insert the *Ngn3* promoter fragment upstream of either DSRed2::c-Myc or eGFP reporters in the pTrip deltaU3 lentiviral

backbones. The lentiviral vector stocks were produced as described before (Castaing 2005).

Production of transgenic mice using lentiviral-mediated gene transfer

The lentiviral vector expressing eGFP under the control of the 5566-bp long fragment of the Ngn3 promoter was injected into the perivitelline space of mouse fertilized eggs as described previously (Lois et al. 2002). The injected eggs were next re-implanted into pseudo pregnant females and the resulting embryos isolated 14.5 days afterwards. They were genotyped with eGFP specific primers (Fw = 5' GACGTAAACGGCCACAAGTTC 3' and Rev = 5'GTCGCCCTCGAACTTCACCTC 3') and fixed in 4% PFA overnight, cryoprotected in 15% sucrose PBS and frozen. Cryo-sections were stained for eGFP (Castaing et al., 2005) and Ngn3 (Zahn et al., 2004), and counterstained with DAPI.

***In situ* hybridization**

For RNA *in situ* hybridization, pancreata were collected, fixed, incubated overnight in 30% sucrose, embedded in cryomatrix, and 18-µm sections were applied to Probe-on Plus slides (Fisher Scientific). Defrosted sections were hybridized overnight with DIG-labeled probes in a medium containing 50% formamide, 10% dextran sulphate, 1 mg/mL yeast tRNA, 0.02% BSA, 0.02% Ficoll, and 0.02% PVP. Tissues were washed successively in 50% formamide, 1X SSC, 0.1% Tween-20 at 70°C for 70 min, and MABT at pH 7.5 (100mMmaleic acid; 150mMNaCl; 0.1% Tween-20) at room temperature for 1 h and blocked in PBS containing 20% inactivated fetal calf serum for 90 min. Anti- DIGantibody (1:2500) was applied overnight in the same solution at room temperature. Tissues were washed thoroughly in MABT for 2 h,

rinsed with NTMT (100 mM NaCl; 100 mM Tris-HCl at pH 9.5; 50 mM MgCl2; 1% Tween-20) for 1 h, stained in a solution containing 350 µg/mL NBT, 175 µg/mL BCIP, rinsed in PBS, and fixed in 4% paraformaldehyde.

Insulin, arginine and liraglutide tolerance tests

Animals of the indicated genotypes were injected subcutaneously with Actrapid insulin (0.75 mU/g – Novo Nordisk - Denmark), intravenously with arginine (5mg - Sigma) or subcutaneously with liraglutide (200 micrograms per kg – Novo Nordisk - Denmark). Following insulin challenge, blood glucose levels were measured as described in the main manuscript. Next to arginine challenge, at each time point, one animal per genotype was sacrificed immediately for serum insulin level determination using RIA (Linco). Lastly, in the case of liraglutide, the latter was injected 30 min prior to glucose challenge. At each time point, three animals per genotype were sacrificed immediately for serum glucose and insulin level determination.

SUPPLEMENTARY REFERENCES

Castaing M, Guerci A, Mallet J, Czernichow P, Ravassard P, and Scharfmann (2005) Efficient restricted gene expression in beta cells by lentivirus-mediated gene transfer into pancreatic stem/progenitor cells. Diabetologia 48: 709–719.

Lee, J.C., Smith, S.B., Watada, H., Lin, J., Scheel, D., Wang, J., Mirmira, R.G., and German, M.S. (2001). Regulation of the pancreatic pro-endocrine gene neurogenin3. Diabetes *50*, 928-936.

Lois C, Hong EJ, Pease S, Brown EJ, Baltimore D. (2002) Germline transmission and tissue-specific expression of transgenes delivered by lentiviral vectors. Science 295: 868–872, 2002.

Ravassard, P. Chatail, F. Mallet, J. & Icard-Liepkalns, C. (1997) Relax, a novel bHLH transcriptional regulator transiently expressed in the ventricular proliferating zone of the developing central nervous system. J. Neurosc. Res. 48, 146-158.

Seymour, P.A., Freude, K.K., Tran, M.N., Mayes, E.E., Jensen, J., Kist, R., Scherer, G., and Sander, M. (2007). SOX9 is required for maintenance of the pancreatic progenitor cell pool. Proc Natl Acad Sci USA, 1865-1870.

Soriano, P. (1999). Generalized lacZ expression with the ROSA26 Cre reporter strain. Nat Genet *21*, 70-71.

Stangé G., Van De Casteele M, and Heimberg H. (2003). Purification of rat pancreatic B-cells by fluorescence-activated cell sorting. Methods Mol Med *83*, 15-22.

Zahn, S., Hecksher-Sørensen, J., Pedersen, I.L., Serup, P., and Madsen, O. (2004). Generation of monoclonal antibodies against mouse neurogenin 3: a new immunocytochemical tool to study the pancreatic endocrine progenitor cell. Hybrid Hybridomics, 385-388.

SUPPLEMENTARY TABLE LEGENDS

Table S1. Quantification of the endocrine cell content alterations in the pancreata of POE::Pdx1cre and POE::Pax6cre animals. A quantitative endocrine marker analysis was performed on pancreata of the indicated genotypes and ages. Using immunohistochemical detection, hormone-expressing cells were counted on every tenth section of pancreas and reported to the pancreatic area estimated *in silico*. The values presented correspond to the averages of hormone-producing cells per square centimeter (also reported in Figure 1Q). Note the age-dependent increase in the β-cell mass at the expense of the other endocrine cell subtypes. ($n>4$, ***$P<0.001$, **$P<0.01$, * $P<0.05$).

Table S2. Quantification of the endocrine cell content alterations in the pancreata of POE::Glucre animals. A quantitative endocrine marker analysis was performed on sections of pancreata of the indicated genotypes and ages Using immunohistochemical detection, hormone-expressing cells were counted on every tenth section of pancreas and reported to the pancreatic area estimated *in silico*. The values presented correspond to the averages of positive cells per square centimeter of pancreas ($n>3$, $P<0.05$, except when labeled with U, Unchanged). Note the loss of α-cells and the concomitant increase in the number of β-galactosidase$^+$ insulin-producing cells and associated markers (Nkx6.1, Pdx1, Glut2, Isl1, HB9) in double transgenic animals, concurrently with an increase in the total endocrine cell number.

Table S3. Real time RT-PCR analysis of selected transcripts in 3- and 6-week old pancreata of different genotypes. The expression of the indicated genes was assayed in pancreatic tissues of POE::Glucre, POE::Glucre supplemented with glucagon, and

glucagon-receptor mutant (GluR-KO) mice using age-matched tissues of WT and POE pancreata as reference (values set at 100%). POE::Glucre, but also GluR-KO pancreata display increased contents of *Ngn3* and *Reg3b* transcripts. Additionally, an augmentation in β-cell-specific transcripts is outlined in POE::Glucre, whereas the expression of the α-cell marker genes is reduced. Importantly, concomitantly with a significant decrease in *Ngn3* and *Reg3b* transcript contents, a reduction in insulin- and glucagon-producing cell numbers (and associated marker genes) is evidenced in POE::Glucre animals supplemented with glucagon. All values are statistically significant ($P<0.05$, $n>2$) versus POE/WT.

Table S4. Assessment of cell contents in 3- or 6-week old pancreata of different genotypes. The counts in cells positive for the indicated genes are reported per square centimeter of pancreatic tissues of POE::Glucre, POE::Glucre supplemented with glucagon, and glucagon-receptor mutant (GluR-KO) mice using age-matched tissues of WT/POE pancreata as reference. It is worth noticing that, in animals ectopically expressing *Pax4* in *glucagon* expression domains or in GluR-KO mice, Ngn3-producing cells reemerge (note for the latter that due to the bias introduced by the high background, this count should be considered as indicative). However, their content becomes significantly reduced in POE::Glucre mice supplemented with glucagon. In the latter case, a concomitant decrease in BrdU-labelled proliferating cell numbers is highlighted (BrdU provided at 5weeks of age, examination a week later). ($n>2$, $^{**}P<0.01$, $^{*}P<0.05$ using the POE/WT genotype as reference; $^{\#\#}P<0.01$, $^{\#}P<0.05$ using the POE::Glucre genotype as reference).

Table S5. The ectopic expression of *Pax4* is sufficient to induce alterations in the endocrine cell content. In order to verify a putative relationship between phenotypic alterations and *Pax4* expression levels, we crossed the five different POE founder lines with Glucre animals. A similar outcome was observed in all cases, resulting in an increase in the insulin-expressing cell content at the expense of the glucagon-producing cell number. Using a combination of GFP intensity examination and real-time PCR analysis, different levels of *Pax4* expression were highlighted in these lines (see thereafter), most probably due to distinct chromosomal integration loci of the transgene. In 3-week-old wild-type mice, *Pax4* is normally produced in β-cells representing 68.21% of endocrine cells. In age-matched double-transgenics, a quantitative analysis demonstrated an expression of *Pax4* in 93.35% of islet cells. Hence, we postulated that, if *Pax4* was to be expressed at the same physiological dosage in double transgenic pancreata as in wild-type, the global *Pax4* pancreatic dosage found in controls should then be relatively increased 1.37-fold (93.35/68.21) in double-transgenic pancreata. However, one also needs to factor in the total endocrine cell number increase upon expression of *Pax4* in α-cells. A careful quantitative analysis demonstrated a 3.67 augmentation of the islet cell count between controls and double-transgenic animals at that age. Thus, the expected increase in *Pax4* dosage, assuming a similar cellular *Pax4* concentration across genotypes, should be of 5.02 (1.37X3.67). Interestingly, in two of our transgenic lines (lines 1 and 4, in red), the global pancreatic increase of *Pax4* expression was found lower than this threshold with values of 4.57 and 3.39, respectively. However, even in these animals, severe alterations in islet cell content were evidenced, indicating that, not only the overexpression of *Pax4*, but also its ectopic expression in glucagon-producing cells, is able to induce a loss of the α-cell phenotype at the profit of β-cell features. All

reported values are statistically significant ($P<0.05$, $n=3$) and were further confirmed by immunohistochemistry (data not shown).

Table S6. *Ngn3* knock-down induces a decrease in the insulin-expressing cell hyperplasia observed in POE::Glucre mice. Animals of POE::Glucre genotype were infected with lentiviruses containing a shRNA either targeting Ngn3 production or a scrambled version. A clear decrease in *Ngn3* and *Reg3b* transcript contents and $Ngn3^+$ cell counts was observed two weeks post-infection (note for the latter that due to the bias introduced by the high background, this count should be considered as indicative). Concurrently, insulin- or glucagon-expressing cell as well as insulin or glucagon transcript contents were found significantly reduced.

Table S7. Perifusion analysis of isolated POE::Glucre isolated islets. Islets of 4- and 12-week-old POE::Glucre mice were isolated by handpicking, following collagenase digestion (0.3 mg/ml) of the pancreata, to study their secretory capacity in a glucose perifusion assay as described by Stangé et al. (2003). Unfortunately, we failed to detect *Pax4* ectopically expressing oversized islets, suggesting that these were overdigested, presumably because of differences in cell-cell adhesion, known to be crucial for islet structure and function, between control and double transgenic mice (Rogers GJ et al., Cell Physiol Biochem, 2007; Caton D et al, Diabetes Metab, 2002; Pipeleers, Experientia, 1984). Obviously, a decrease in digestion time/collagenase concentrations would not have permitted proper islet isolation. We anyway perifused the islets and observed no difference in islet function of younger animals for all the genotype analyzed. However, in older counterparts, we did detect a decrease in the glucose-stimulated insulin release, albeit not significant. It should be notice that such

a lack of significance might be attributed to the loss of oversized islets induced by experimental conditions.

SUPPLEMENTARY FIGURE LEGENDS

Figure S1. Generation of animals able to conditionally and ectopically express the *Pax4* gene. (A) Schematics depicting the targeting vector prior to (top) and following (bottom) homologous recombination of the two LoxP sites induced by the phage P1 cre recombinase. β-Galactos., β-galactosidase. (B-C) Visual examination under fluorescent light of an E10.5 embryo and adult pancreas, both representative of Cre-negative animals. (D-G) POE exocrine and endocrine (note the islet outlined in D-E) cells do not express β-galactosidase as demonstrated through LacZ staining (whereas GFP staining is present in a majority of pancreatic cells; D-E). Importantly, β-galactosidase activity is found restricted to the islet of Langerhans in age-matched POE::Pax6cre pancreata (F), whereas almost all pancreatic cells are β-galactosidase-positive in POE::Pdx1cre pancreata (G).

Figure S2. The forced expression of *Pax4* in *Pax6* or *Pdx1* expression domain results in islet overgrowth and increased β-cell mass. Representative islets of POE (A and Figure 1E) and POE::Pax6cre/Pdx1cre (B and Figure 1G) pancreata stained with the indicated antibodies and observed using the same magnification. Note the dramatic islet size augmentation in POE::Pax6cre/Pdx1cre pancreata as a result of a drastic increase in β-cell number (B). A decrease in glucagon-expressing numbers is also highlighted in pancreata of animals ectopically expressing *Pax4* (B).

Figure S3. The forced expression of *Pax4* in *Pax6* or *Pdx1* expression domain results in islet overgrowth and increased β-cell mass (low magnification). Representative sections of POE (A) and POE::Pax6cre/Pdx1cre (B) pancreata stained with anti-insulin antibodies and observed using the same magnification. Note the

remarkable islet size augmentation in POE::Pax6cre/Pdx1cre pancreata (B) as a result of a drastic increase in β-cell numbers.

Figure S4. Characterization of a newly developed anti-Pax4 antibody. Using immunohistochemistry, an anti-Pax4 antibody (Wang et al., 2008) raised in rabbit was tested in wild-type (A-B) and Pax4-depleted (C-D) adult islets. In the wild-type situation, Pax4 is clearly detected in most β-cells (A), but not in α-cells (B), nor in δ- or PP-cells (see Figure S5). In *Pax4* mutant pancreas, characterized by a loss of β- and δ-cells at the benefit of glucagon-expressing cells, Pax4 detection is expectedly negative (C-D). The same observation was also made in *Ngn3* mutants lacking endocrine cells (data not shown). Each picture is representative of at least 3 independent animals.

Figure S5. POE, POE::Pdx1cre and POE::Pax6cre insulin-producing cells express *Pax4*. An anti-Pax4 antibody (Wang et al., 2008) was used to study *Pax4* expression in adult pancreata together with the indicated endocrine hormones. Pax4 is clearly detected in most insulin-expressing cells both in POE (A-D) and POE::Pax6cre islets (E-H), whereas α-, δ- and PP-cells are found devoid of Pax4 protein (B-D, F-H, respectively). Interestingly, the vast majority of POE::Pdx1cre pancreatic cells are found positive for Pax4 (I-L). For the purpose of clarity, the magnification of double-transgenic islets is five times reduced compared to controls. Each picture is representative of at least 4 independent animals.

Figure S6. Assessment of *Pax4* transcripts in adult wild-type and POE::Pax6cre pancreata. Due to conflicting reports concerning the expression of *Pax4* in adult β-

cells, we attempted to amplify *Pax4* mRNA using classical RT-PCR. Such an approach was unsuccessful, most likely due to the presence of numerous secondary structures within the *Pax4* mRNA (Figure S7) and/or its weak expression. However, using a mixture of eight antisense oligonucleotides (depicted as red arrows in A) designed to cover the whole *Pax4* mRNA for the reverse transcription step (instead of classical oligo-dT oligonucleotides), subsequent PCR reactions were successful (a β-actin control set being included). The location of the oligonucleotides used for these is indicated as blue (forward) and red (reverse) arrows. To test whether *Pax4* transcripts were present in wild-type and POE::Pax6cre pancreata, we first used 45 cycles of elongation for the eight different PCR reactions. In both instances, similar results were obtained with a clear detection of PCR products. Semi-quantitative PCR reactions were next carried out using 30 cycles of elongation. Representative pictures are presented and demonstrate a mild expression of *Pax4* in wild-type pancreata that is strongly increased in double-transgenic animals. A list of the different oligonucleotides used is provided in B. WT, wild-type; OE, POE::Pax6cre.

Figure S7. *Pax4* mRNA predicted secondary structure. The putative presence of secondary structures within the *Pax4* mRNA was revealed using the RNAfold program (http://mobyle.pasteur.fr/cgi-bin/MobylePortal/portal.py?form=rnafold). The plot of the predicted secondary structures calculated based on minimum free energy demonstrates that *Pax4* mRNA is exceptionally structured through matching of complementary nucleotides. This may be the cause of the difficulties encountered with classical RT-PCR, but also explains the lack of working antisense probe for *in situ* hybridization purposes. Note that this plot allows online close-up viewing.

Figure S8. Cre activity faithfully recapitulates *glucagon* expression in Glucre mice. Assessment of Cre recombinase activity in glucagon promoter-Cre (Glucre - Herrera, 2000) mice crossed with Rosa26 promoter-LoxP-STOP-LoxP-β-Galactosidase reporter animals (Soriano, 1999). Cre activity was visualized using LacZ staining (A-B) at the indicated magnifications and compared to glucagon expression assayed using immunohistochemistry on a consecutive section (C). A similar expression pattern was observed for glucagon and β-galactosidase thereby confirming previously published results (Herrera, 2000). Each picture is representative of at least 3 independent animals.

Figure S9. Analysis of 6-week old POE::Glucre pancreata in relation to different marker genes and proliferation labels. Serial sections of POE::Glucre animals treated with BrdU and examined a week later (F) or not were stained using the indicated antibody combinations. While Ngn3-expressing cells were found mostly located adjacent to the islet (A), Pax4- (B), Pdx1- (C) and β-galactosidase- (E) producing cells were detected exclusively within the islet of Langerhans. Only few glucagon$^+$/Pax4$^+$ (inlet in B) or glucagon$^+$/β-galactosidase$^+$ cells (inlet in E), and even fewer glucagon$^+$/insulin$^+$ (inlet in G), were observed in POE::Glucre pancreata, indicating an extremely rapid transition between glucagon$^+$ and insulin$^+$ phenotypes. Importantly, most proliferating cells were detected within the duct epithelium (D, F) or the islet domain adjacent to ducts (F). The duct epithelium and lining were found uniformly positive for GFP (H-K), suggesting that *Pax4* ectopic expression mostly occurs within the islet (B, E).

Figure S10. An increase in Pax4 dosage does not induce β-cell proliferation. Endocrine cell counts from adult wild-type and POE::Inscre animals were assessed after immunostaining against all four hormones. No statistically significant difference could be found between both genotypes (n=7, all values are expressed as means ± standard error of the mean).

Figure S11. Assessment of *Ngn3* expression using two different anti-Ngn3 antibodies. *Ngn3* expression was determined using a mouse anti-Ngn3 antibody (Zahn et al., 2004; A-B, E-H) and a goat anti-Ngn3 antibody (provided by M. Sander's laboratory (Seymour et al., 2007; C-D, G-H). Staining of POE (Cre^-, G-H), POE::Pdx1cre/POE::Pax6cre/POE::Glucre (Cre^+, A-F) pancreata suggest *Ngn3* expression in the pancreatic duct lining from animals ectopically expressing *Pax4*.

Figure S12. Detection of *Ngn3* expression in POE::Glucre pancreata using *in situ* hybridization. *Ngn3* expression was assayed using two antisense probes (constructed by G. Gradwohl and P. Ravassard). (A-F) Albeit extremely difficult on adult tissues, this approach allowed us to detect few labeled cells in ductal structures in A and D (serial 18µm sections). Photographs of the same sections counterstained with propidium iodide are provided in B and E, and merged pictures in C and F, respectively. Note the expression of *Ngn3* in the cytoplasm of ductal cells (inlets in C, F). Bear in mind that due to thickness of the section (18µm) and curved nature of the duct tubes, the lumen of the latter is not always distinguishable (D-F). (G-I) Using a sense probe, we did not detect any labeled cells.

Figure S13. Characterization of *Ngn3* expression in POE::Glucre pancreata using a lentiviral approach. Lentiviruses encompassing a 5566-bp long fragment of the mouse *Ngn3* promoter (orthologous region of the human *Ngn3* promoter characterized in Lee et al., 2001) driving the expression of a DsRED2::c-Myc cassette (see supplementary experimental procedures) were used to infect the pancreata of POE::Glucre (C-N) or POE (A-B) animals as previously described (Xu et al., 2008). Due to the technical limitations previously discussed, the transgene was detected using an anti-c-Myc antibody. Control pancreata were found negative for c-Myc detection (A-B), whereas variable results were obtained within the same POE::Glucre pancreas, ranging from ducts negative for c-Myc (C-D), to ducts displaying different numbers of c-Myc-labeled cells (E-N), such discrepancies most likely originating from different levels of infection. Note that the specificity of the *Ngn3* promoter employed was also tested (Figure S16).

Figure S14. Characterization of *Ngn3* expression in POE::Glucre pancreata using a lentiviral approach (serial sections). The duct displayed in Figure S13M-N was assayed on consecutive sections for c-Myc (B-F) and Ngn3 (A) expression. C-Myc-marked cells were found mostly located within the ductal lining adjacent to the islets (B-F), a locus were *Ngn3*-producing cells where detected (A). A' and B' correspond to A and B, respectively, visualized for residual GFP expression and DAPI.

Figure S15. Assessment of the specificity of the 5.6 kb fragment of the mouse *Ngn3* promoter. (A-L) To determine whether the 5566-bp long fragment of the mouse *Ngn3* promoter was sufficient to recapitulate *Ngn3* expression in the pancreas,

a lentiviral vector expressing the *eGFP* reporter gene under the control of this promoter element was injected in the perivitelline space of mouse fertilized eggs. The resulting eggs were reimplanted in pseudo pregnant females and the derived embryos isolated 14.5 days later. Eleven transgenic founder embryos were obtained and co-stained to detect both *Ngn3* and *eGFP* expression. Briefly, using TSA amplification, 12μm cryosections were stained with the anti-Ngn3 mouse monoclonal antibody (red, B-C, E-F, H-I, K-L) from and according to Zahn et al. (2004). Concomitantly, eGFP expression was revealed with a rabbit polyclonal anti-GFP antibody (green, A, C, D, F, G, I, J and L) as described by Castaing et al. (2005). (A-C) Pancreata of wild-type embryos derived from re-implanted injected eggs, are expectedly eGFP-negative (A), whereas scattered Ngn3-labelled positive cells are visualized (B-C). (D-L) The analysis of representative sections of 3 pancreata of *eGFP*-expressing founders (6 out of 11) indicates that the vast majority of *Ngn3*-expressing cells are eGFP positive thereby demonstrating the specificity of the 5566-bp long mouse Ngn3 promoter fragment (yellow, F, I and L).

Figure S16. Reactivation of *Ngn3* expression in *glucagon-receptor*-deficient pancreata. Representative islet of adult *glucagon-receptor*-deficient animals assayed for Ngn3 (A) and counterstained with DAPI (B). A merged picture is displayed in C. Note the detection of few Ngn3-labelled cells in this genotype, whereas control age-matched counterparts are negative for Ngn3 (Figure S11G-H). A quantitative analysis of this data is presented in Table S4.

Figure S17. *In vivo* assessment of β-cell function in 10-week old *Pax4*ectopically expressing pancreata. (A) Through a combination of glucose challenge and

circulating insulin measurements, an impairment in β-cell function is outlined in 10-week old POE::Glucre/POE::Pdx1cre/POE::Pax6cre animals: these exhibit a worsen and extended response time to glucose injection that may be explained by a decreased insulin secretion as compared to POE control counterparts. Note that 600mg of glucose per dl of blood correspond to the maximal value detectable by our glucose monitoring system. (B) For the purpose of comparison, a copy of the graph displayed in Figure 2U is included. Aiming to study the islets of double transgenic animals, these were isolated. However, due to the experimental conditions used, we noticed a disaggregating of the islets (Table S7) and therefore turned to an *in vivo* approach: (C) To determine the overall responsiveness to insulin, an insulin challenge was performed in animals of the indicated genotypes and ages. Importantly, we did not observe any significant modification of the glycemia in older POE::Glucre animals (in green) as compared to their younger counterparts (red) or controls animals (blue), suggesting a late-onset insulin insensitivity (n=3, **P<0.01, *P<0.05 using the lowest glycemia value within the same genotype (40 min post-challenge) as reference).

(D-F) Aiming to also assay β-cell function, we treated POE::Glucre animals of the indicated genotypes and ages with two insulin secretagogues, arginine and liraglutide (a long-acting GLP-1 analog – Novo Nordisk - Denmark). It is interesting to notice that both were able to elicit an insulin secretion from hyperplastic 10-week old POE::Glucre β-cells, albeit lower than seen in younger animals (D, F). As important was the observation that liraglutide also promoted an improved glucose clearance upon glucose challenge (E), indicating that despite their altered sensitivity to glucose, older β-cells retain the ability to secrete insulin (n=3, **P<0.01, *P<0.05 using the 10-week old POE::Glucre genotype as reference).

SUPPLEMENTARY MOVIE LEGENDS

Movie S1. Duct structures are tightly connected to the clusters of glucagon-expressing cell observed in double-transgenic animals. Pancreata from POE::Glucre, POE::Pax6cre and POE::Pdx1cre genotypes were sectioned (10µm thickness). Every third section was stained with an anti-glucagon antibody and photographed. Using the Amira software (Mercury), the pictures were aligned and movies allowing to flip back and forth between the different pictures, were generated (z-stack). A representative movie for all three genotypes is presented in A. The same pictures were used to generate a second movie were the duct lumen has been highlighted in blue (B) to better outline the connection between the focus of glucagon-expressing cells and duct structures.

Collombat et al., 2009 - Table S1

Quantification of the endocrine contents in POE::Pdx1cre and POE::Pax6cre pancreata (average cell counts per square centimetre of pancreas)

		POE/ WT	POE::Pdx1cre	POE::Pax6cre
P24h	Insulin	127±9	165±19 (+29%)**	171±12 (+35%)**
	Glucagon	43±8	9±1 (-79%)**	6±1 (-86%)**
	Somatostatin	25±6	11±2 (-56%)**	10±2 (-60%)**
	PP	8±2	2±0 (-75%)*	6±1 (U)
6 weeks	Insulin	278±33	1245±101 (+350%)***	1022±99 (+267)***
	Glucagon	93±23	27±9 (-70%)**	22±10 (-76%)**
	Somatostatin	62±12	31±13 (-50%)**	36±14 (-42%)**
	PP	9±2	5±3 (U)	3±1 (-66%)*
Short before death	Insulin	299±56	1702±169 (+470%)***	1799±125 (+501%)***
	Glucagon	88±22	14±6 (-84%)**	9±7(-90%)**
	Somatostatin	49±8	12±5 (-76%)**	14±8 (-72%)**
	PP	18±7	3±2 (-83%)*	2±1 (-89%)*

Collombat et al., 2009 - Table S2

Pax4 ectopic expression promotes glucagon-expressing cells to acquire a β-cell phenotype

Age	E20		6weeks		12weeks	
	POE	*POE::Glucre*	*POE*	*POE::Glucre*	*POE*	*POE::Glucre*
Insulin	133±12	176±9 (+24%)	267±20	1633±187 (+512%)	299±29	2764±356 (+824%)
β-galactosidase	1±2	51±13	*0*	1444±167	*0*	2612±289
Glucagon	58±6	15±7 (-73%)	83±13	17±11 (-79%)	111±45	12±9(-89%)
Somatostatin	21±4	17±5 (U)	35±8	31±14 (U)	42±12	40±19 (U)
PP	3±1	2±0 (U)	8±6	7±5 (U)	10±9	8±7 (U)
Arx	74±10	18±9 (-74%)	99±10	36±12 (-64%)	114±18	24±15 (-79%)
Nkx6.1	129±14	172±13 (+25%)	259±21	1672±223 (+545%)	258±31	2865±401 (+1009%)
Pdx1	130±10	164±9 (+21%)	253±33	1567±201 (+518%)	279±32	2537±505 (+810%)
Glut-2	128±8	177±8 (+28%)	241±33	1616±157 (+570%)	276±44	2969±356 (+974%)
HB9	126±11	171±11 (+26%)	252±28	1644±335 (+552%)	319±48	2748±287 (+760%)
Brn4	66±9	14±6 (-78%)	78±9	22±14 (-72%)	107±23	19±4 (-82%)
Nkx2.2	187±18	192±11 (U)	334±41	1439±201 (+330%)	425±41	2714±188 (+538%)
Isl1	214±18	208±19 (U)	385±50	1757±176 (+356%)	453±30	3152±667 (+595%)
Pax6	216±25	203±31 (U)	390±38	1886±331 (+383%)	460±28	3146±491 (+584%)
Islet area	100%	99.8%	100%	+381.1%	100%	+583.2%
Glucose levels	-	-	91mg/dl	121mg/dl (+33%)	101mg/dl	351mg/dl (+248%)
Life expectancy	normal	3-12weeks	normal	3-12weeks	normal	3-12weeks

Collombat et al., 2009 - Table S3

Real time RT-PCR analysis of selected transcripts in animals of different genotypes

	3week old animals		6week old animals	
	POE::Glucre	GluR-KO	POE::Glucre	POE::Glucre +glucagon
Insulin	423±24%	37±9%	559±82%	285±52%
Glucagon	22±11%	1350±98%	27±15%	18±9%
Pax4	608±98%	41±4%	514±87%	555±91%
Ngn3	1244±89%	623±44%	1120±159%	475±81%
Reg3b	623±22%	1070±109%	724±93%	434±63%
Arx	27±6%	1480±121%	17±9%	15±10%
Pdx1	274±39%	31±8%	502±85%	279±62%
Nkx6.1	398±51%	40±4%	491±60%	183±20%

Collombat et al., 2009 - Table S4

Quantification of cell numbers expressing selected genes in animals of different genotypes (average cell counts per square centimetre of pancreas)

	3week old animals			6week old animals		
	POE/WT	POE::Glucre	GluR-KO	POE/WT	POE::Glucre	POE::Glucre +glucagon
Insulin	182±71	821±107**	59±33*	267±20	1103±128**	394±132**$^{\#\#}$
Glucagon	72±21	32±26	789±137**	83±13	19±6**	6±4**$^{\#}$
Ngn3	-	53±9	21±8	-	63±15	38±11$^{\#}$
BrdU (1week)	-	-	-	23±5	57±9**	28±7$^{\#}$

Collombat et al., 2009 – Table S5

Quantification of transcript contents in the five different POE::Glucre mouse lines

	POE- -Line 1 to 5-	POE::Glucre -Line 1-	POE::Glucre -Line 2-	POE::Glucre -Line 3-	POE::Glucre -Line 4-	POE::Glucre -Line 5-
Insulin	100%	+383%	+352%	+417%	+336%	+399%
Glucagon	100%	-91%	-89%	-96%	-79%	-93%
Somatostatin	100%	U	U	U	U	U
PP	100%	U	U	U	U	U
Pax4	100%	+457%	+834%	+2006%	+339%	+2776%

Collombat et al., 2009 - Table S6

Assessment of the effect of *Ngn3* knock-down in POE::Glucre animals

	Transcript relative expression		Absolute cell count/cm^2	
	POE::Glucre+ Scramble	POE::Glucre+ shRNA	POE::Glucre+ Scramble	POE::Glucre+ shRNA
Ngn3	100±10%	33±7%**	55±12	21±7 (-61%) **
Insulin	100±4%	68±8%*	1340±172	402±61 (-70%) **
Glucagon	100±12%	43±11%*	23±7	7±5 (-69%) *
Reg3b	100±13%	44±16%**	-	-

Collombat et al., 2009 - Table S7

Assessment of isolated islet properties using perifusion in POE::Glucre animals

	% of insulin released reported to the total insulin cell content/2h			
Glucose stimulation:	2.5mM	7.5mM	20mM	20mM+glucagon
3-week old				
Control	0.7±0.2	0.8±0.1	8.2±0.2	8.9±1.1
POE::Glucre	0.8	0.8	9.4	10.6
12-week old				
Control	0.7±0.1	1.0±0.3	10.4±1.7	9.5±0.8
POE::Glucre	0.5±0.0	0.7±0.3	6.9±0.7	6.6±1.2

Collombat et al., 2009 - Figure S1

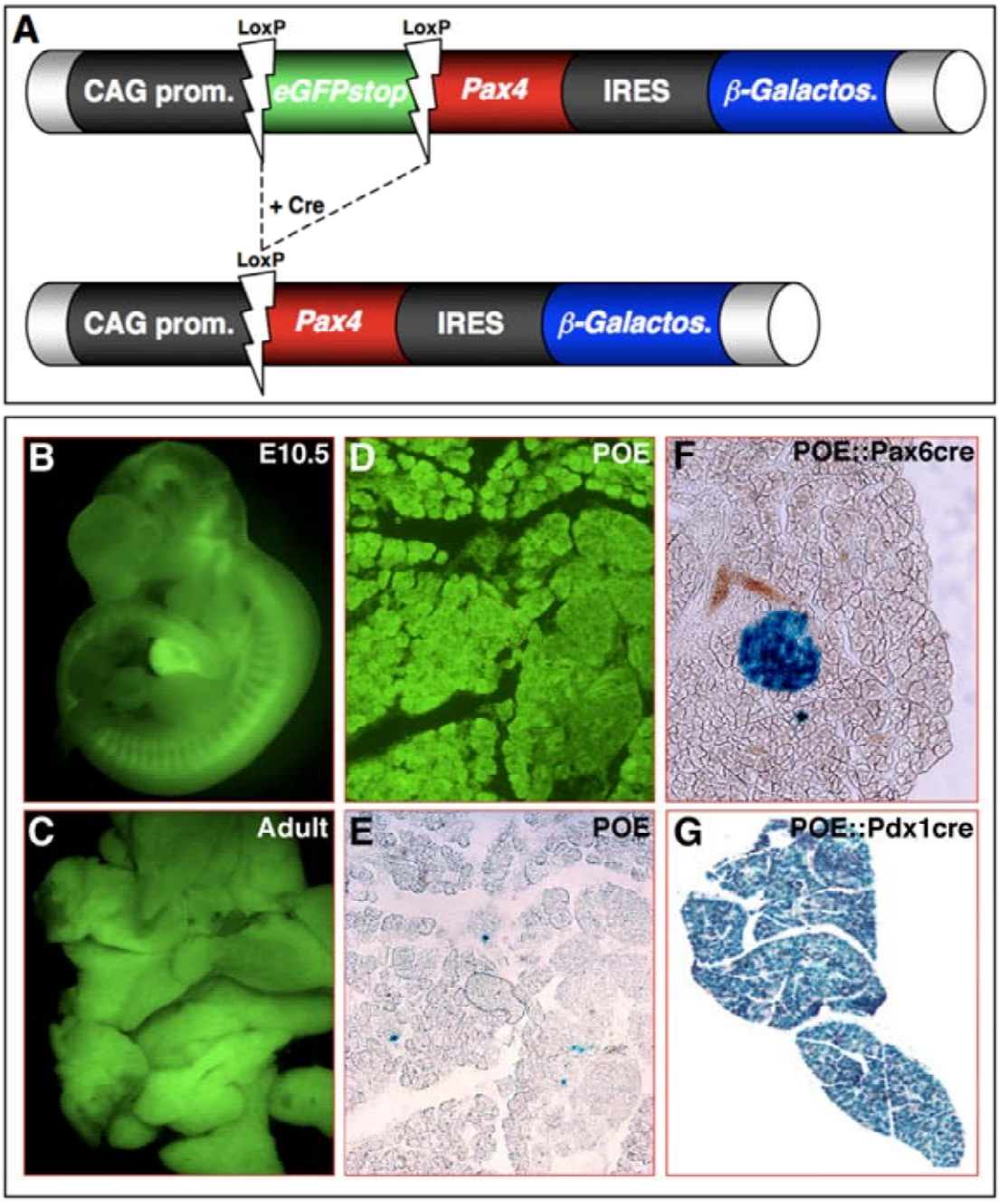

Collombat et al., 2009 - Figure S2

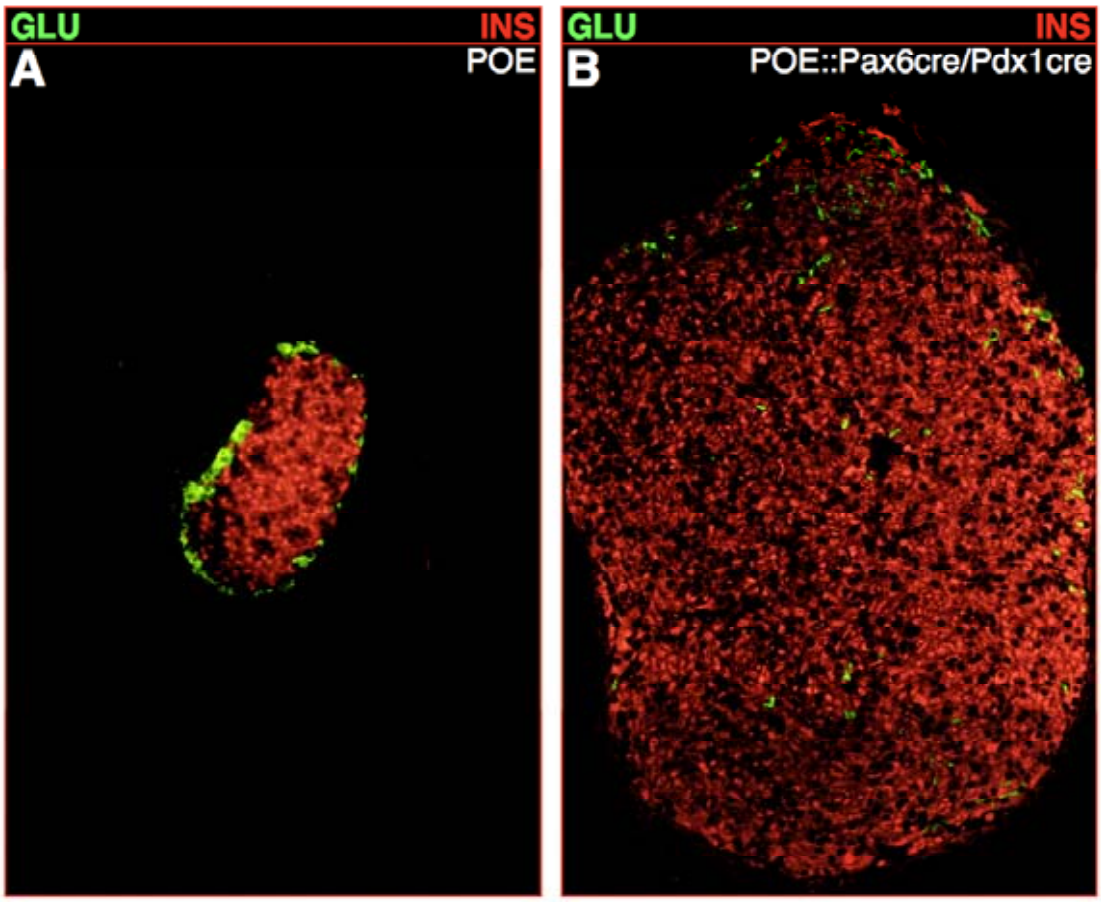

Collombat et al., 2009 - Figure S3

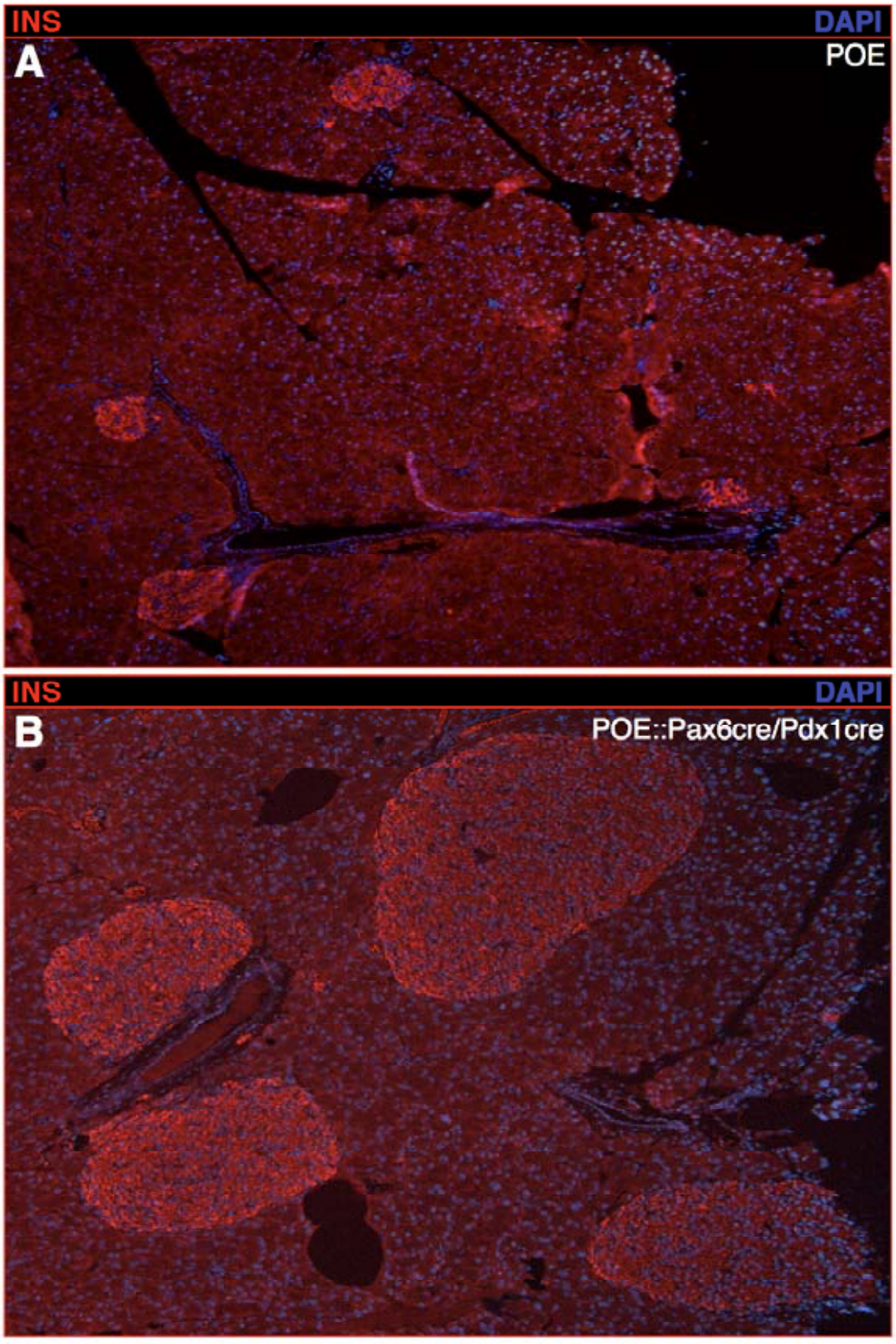

Collombat et al., 2009 - Figure S4

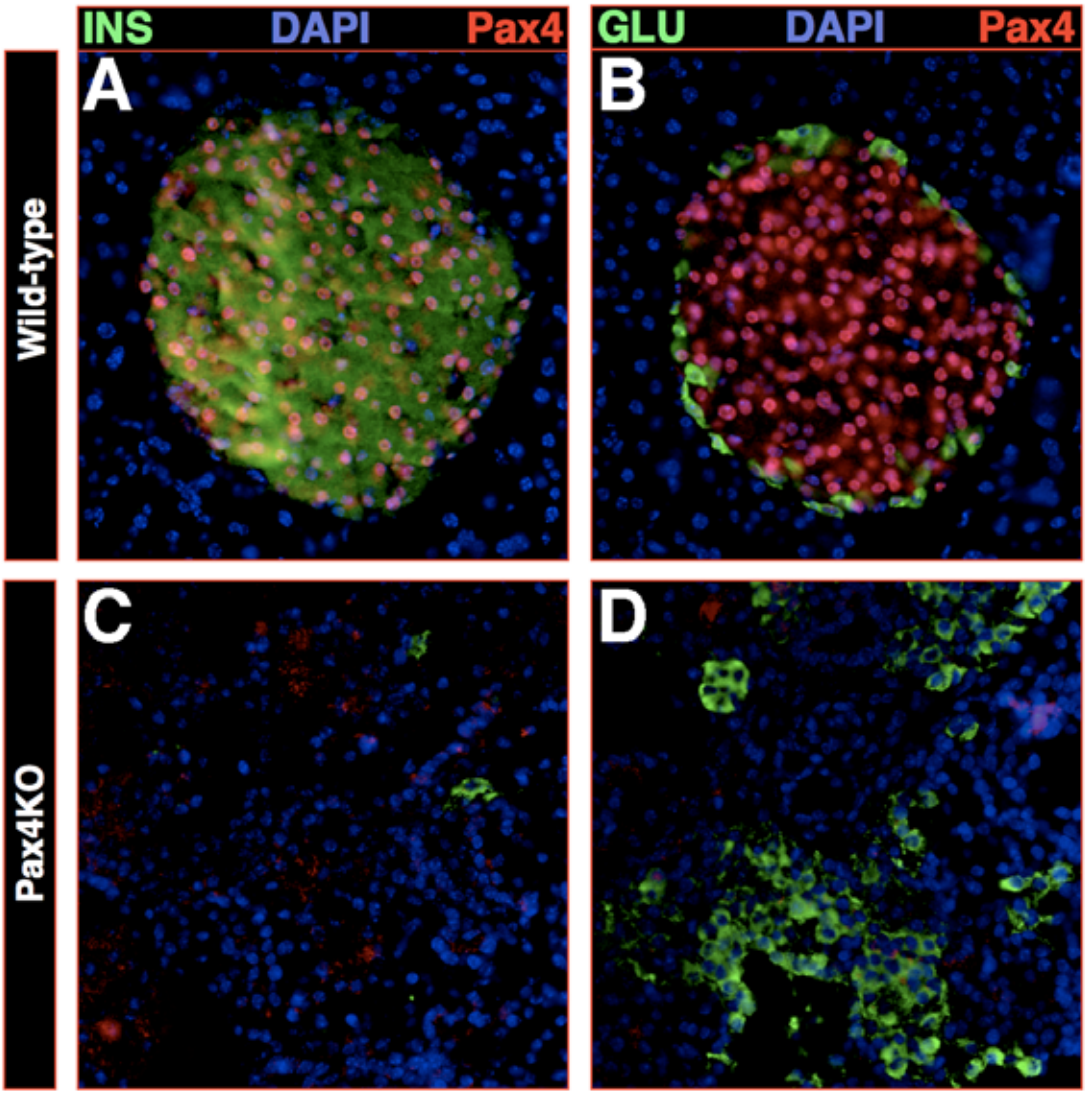

Collombat et al., 2009 - Figure S5

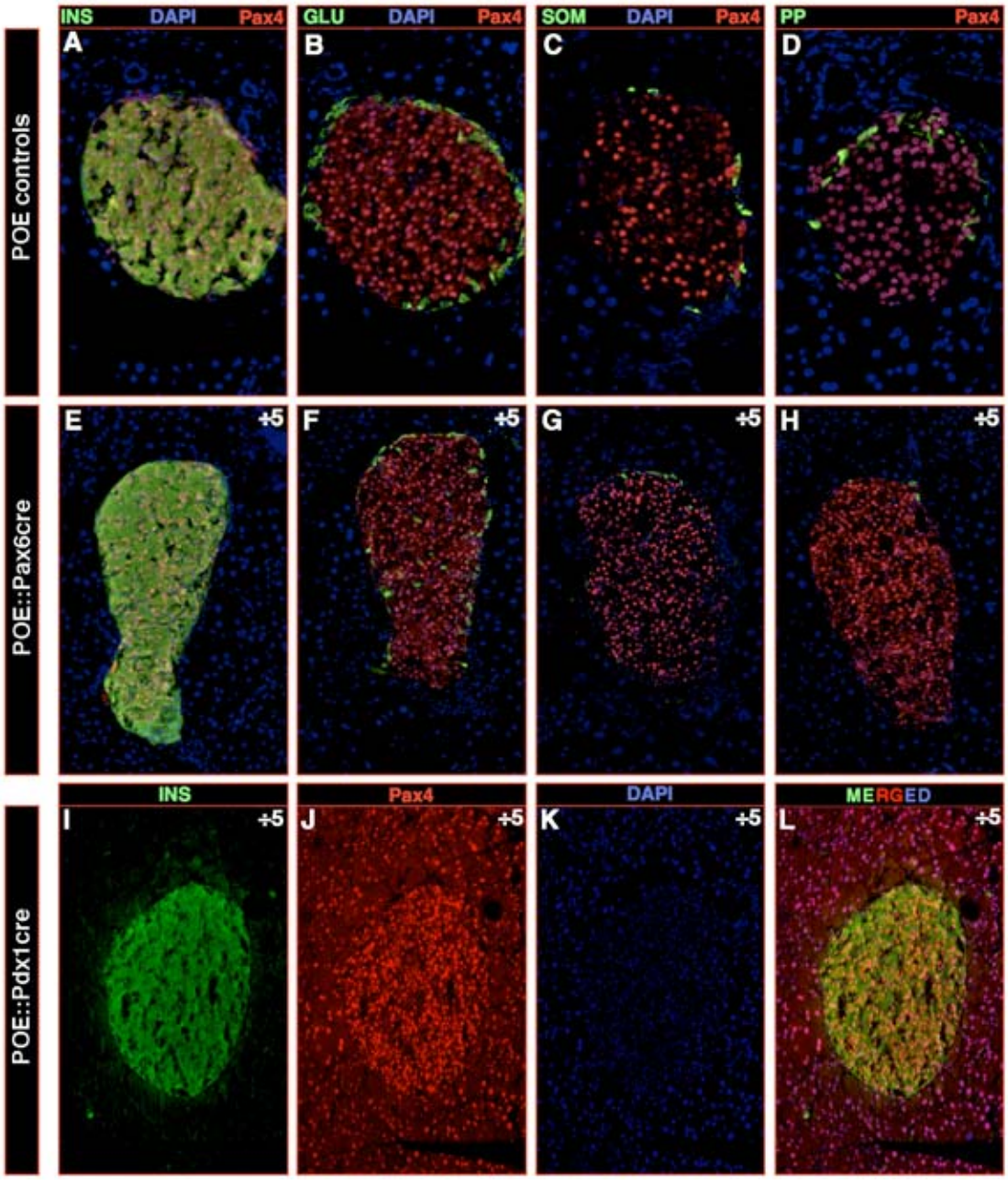

Collombat et al., 2009 - Figure S6

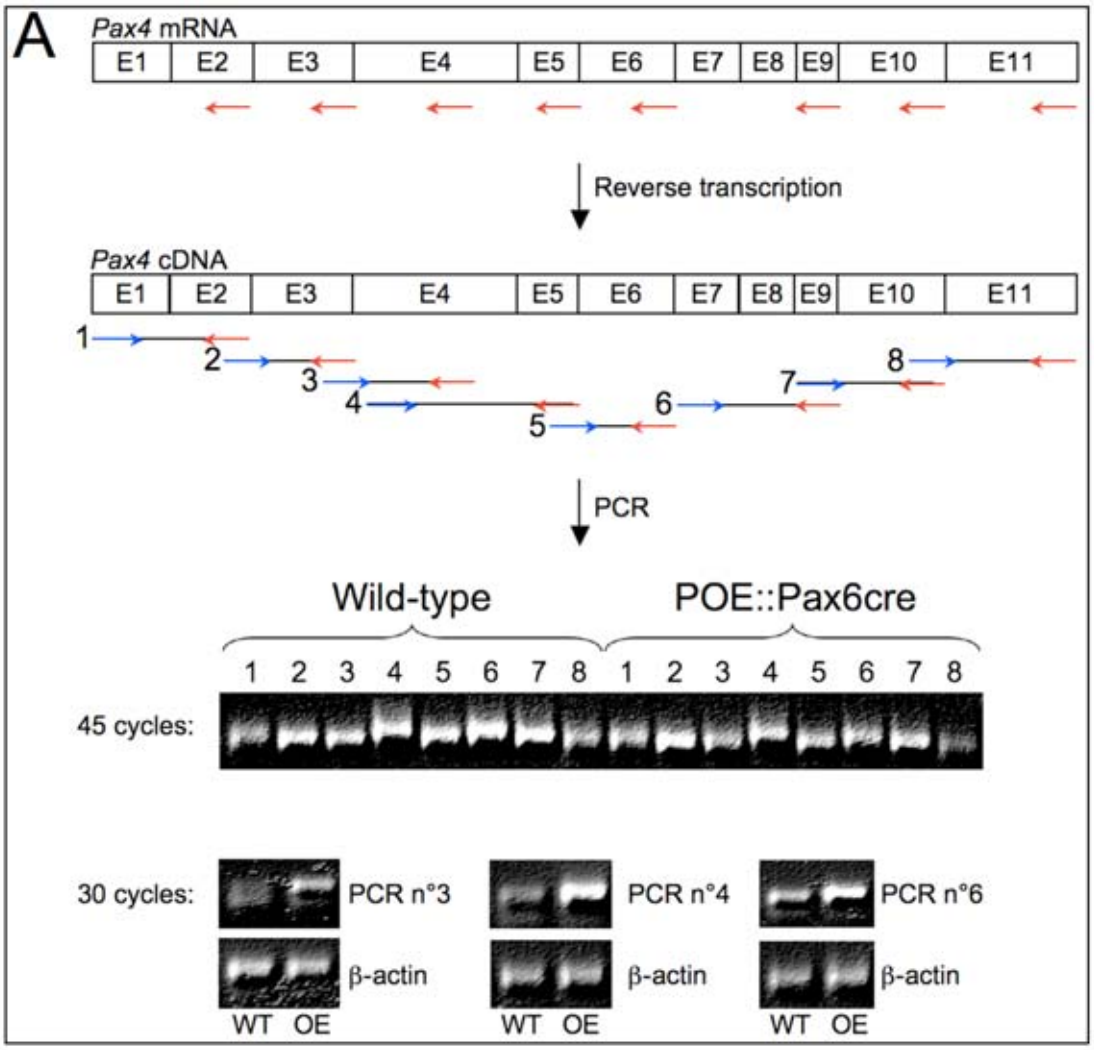

B

Oligonucleotide set	Forward (5'-3')	Reverse (5'-3')	Amplicon (bp)
1	AGCTGGAGGCTGTTACAAGACCAGACCACCAGCAA	TTCTGTGAGGAGTACCAGTGTGAAGCATGCAGCAG	207
2	TTCTGTGAGGAGTACCAGTGTGAAGCATGCAGCAG	GATGCGACCCTGTGACATTTCACGGAGCCTTAAGG	173
3	GATGCGACCCTGTGACATTTCACGGAGCCTTAAGG	AGCAAACCACGTCTGGCCACACCTGCTGTGGTGGC	152
4	CAAGATCCTAGGACGCTACTACCGCACAGGTGTCT	GAAGACCAGAGCTTGCACTGGACTCAACTCAGATC	275
5	GAAGACCAGAGCTTGCACTGGACTCAACTCAGATC	TATCTTCTCCCCGGGACAAGCCGAGGCACTGGAGA	166
6	GTTTCAGCGTGGGCAGTATCCAGATTCAGTGGCCC	TGACAGTACCAAAAAATTCTCCAGGGATCATCTCT	210
7	TGACAGTACCAAAAAATTCTCCAGGGATCATCTCT	TGACACCTCATCCCAGGCCTATCTCCAACCCTACT	182
8	TGACACCTCATCCCAGGCCTATCTCCAACCCTACT	ACCCATCCTGTGCATCATCTGATTGGAGGCCCAGG	139

Collombat et al., 2009 - Figure S7

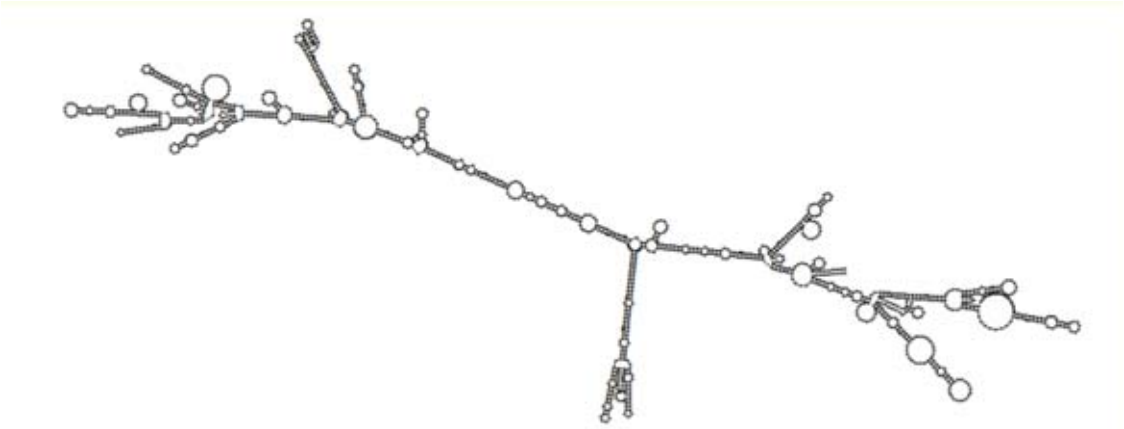

Collombat et al., 2009 - Figure S8

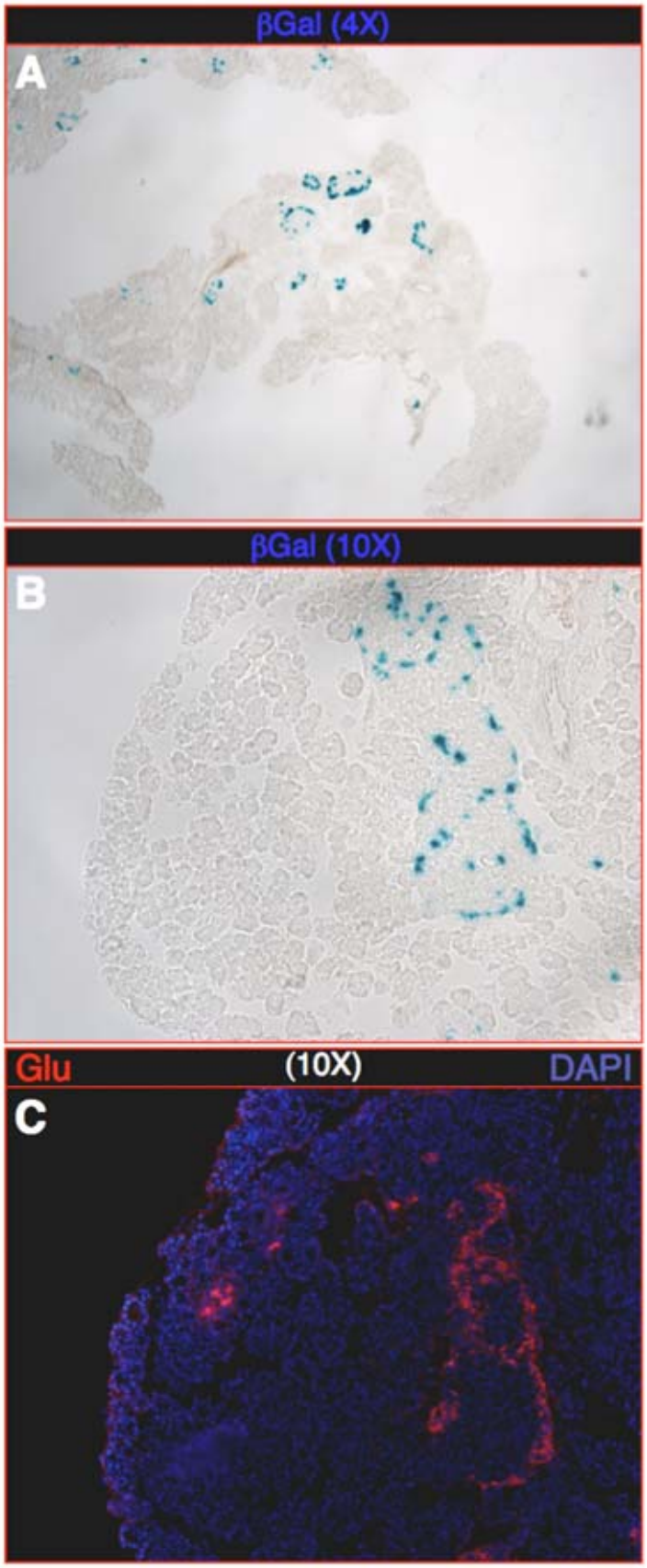

Collombat et al., 2009 - Figure S9

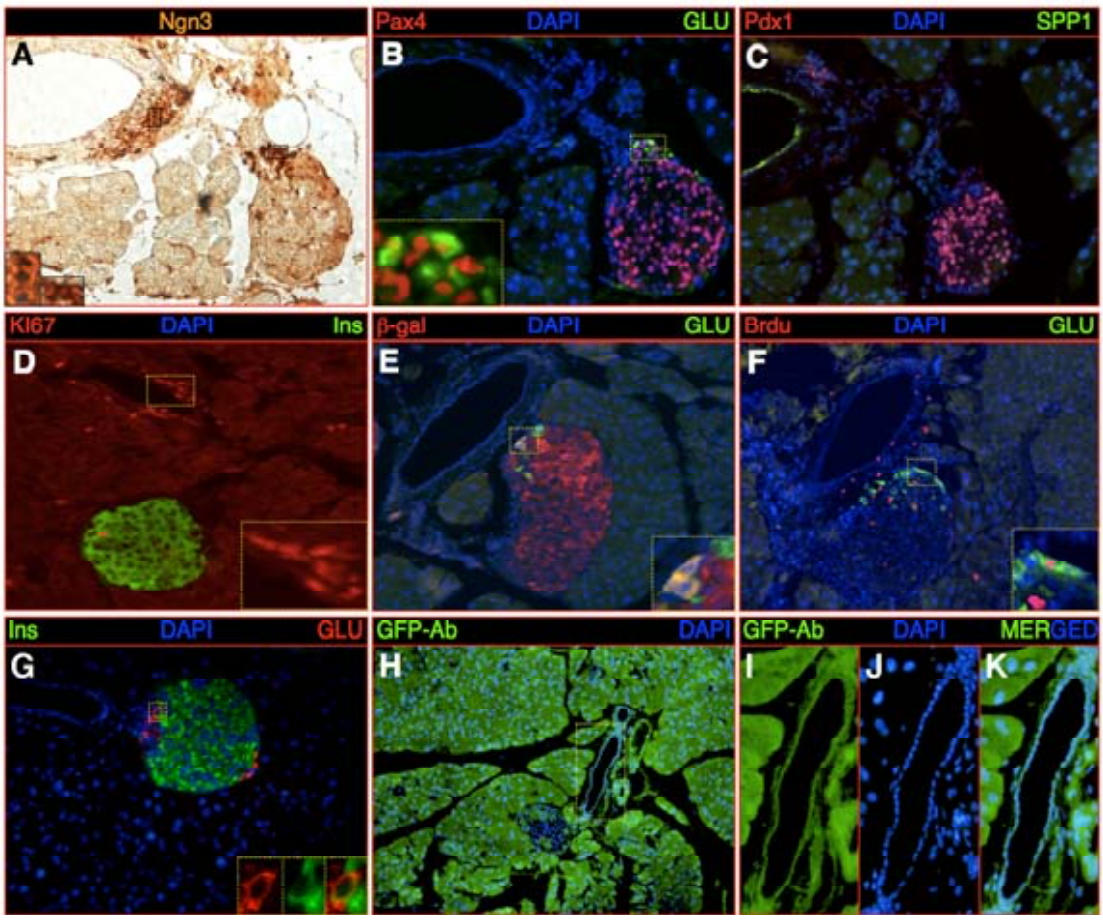

Collombat et al., 2009 - Figure S10

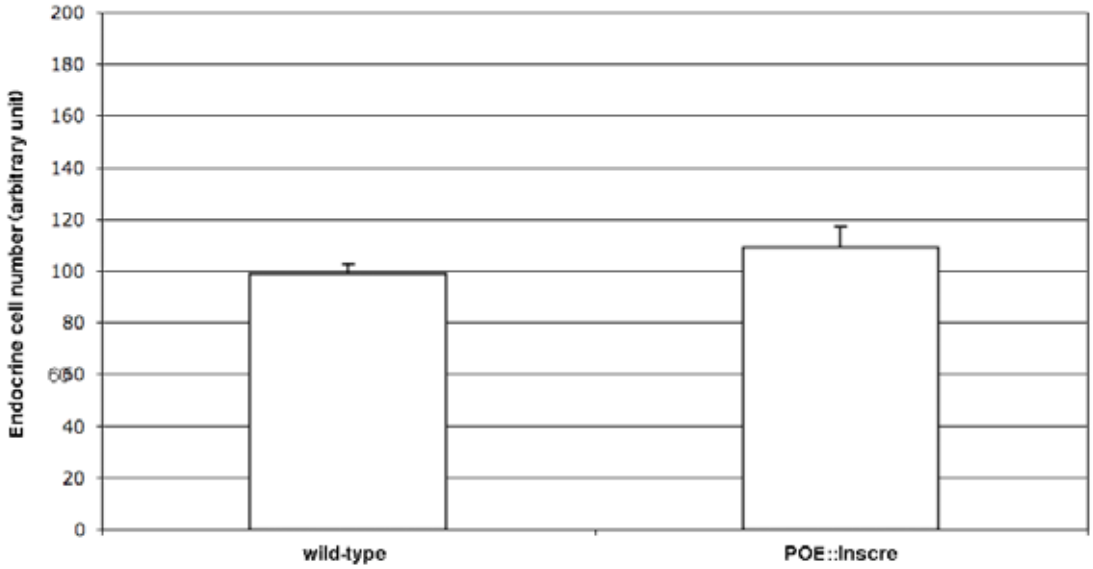

Collombat et al., 2009 - Figure S11

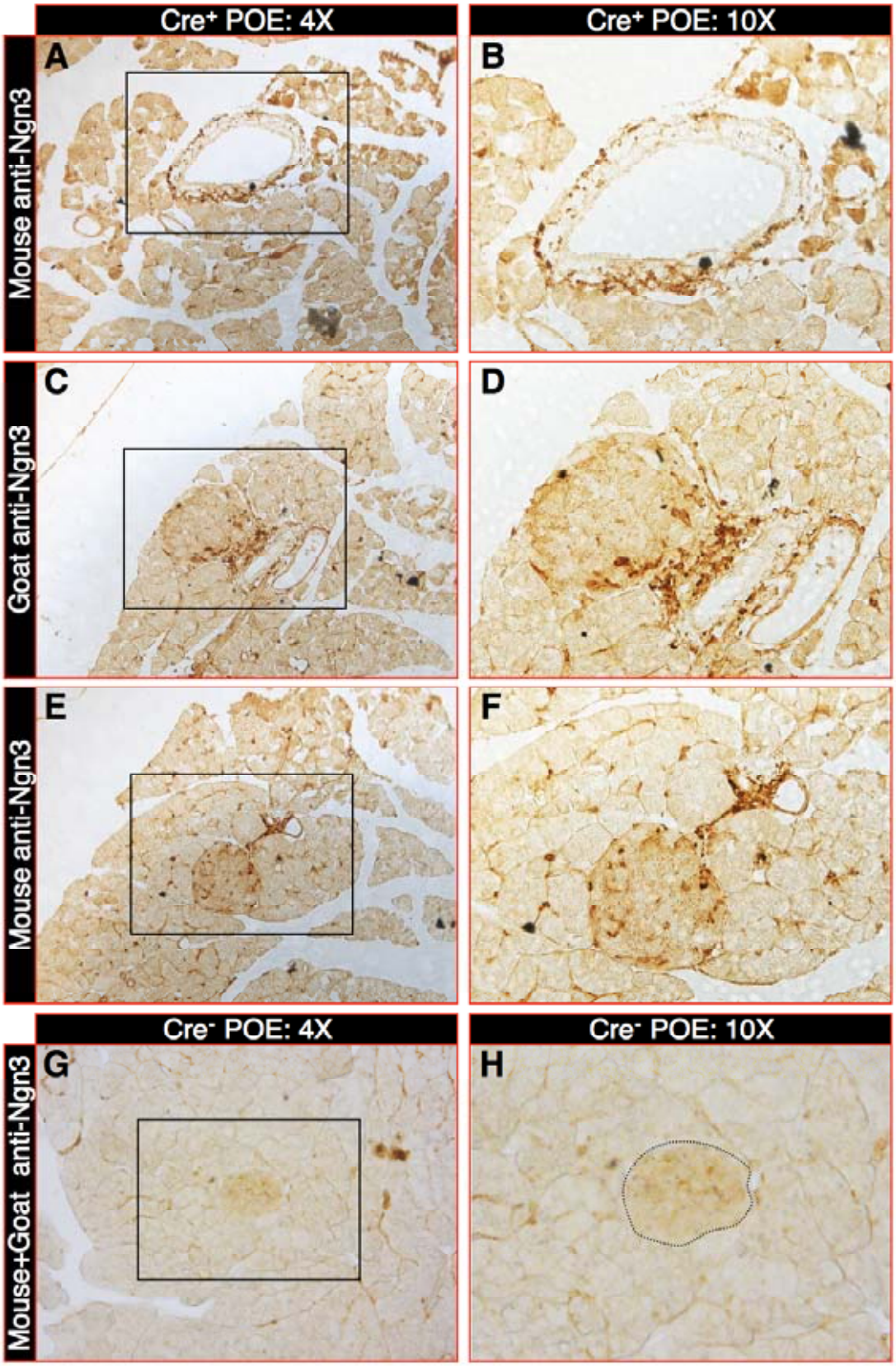

Collombat et al., 2009 - Figure S12

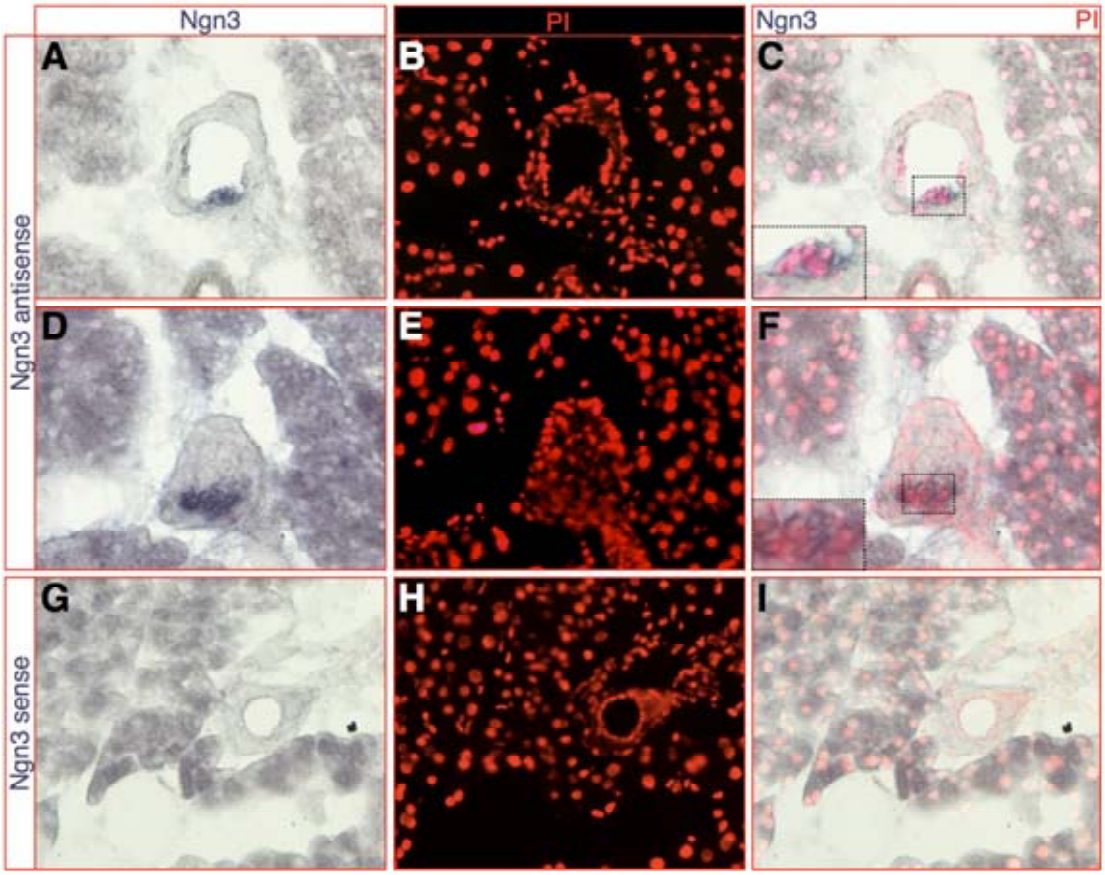

Collombat et al., 2009 - Figure S13

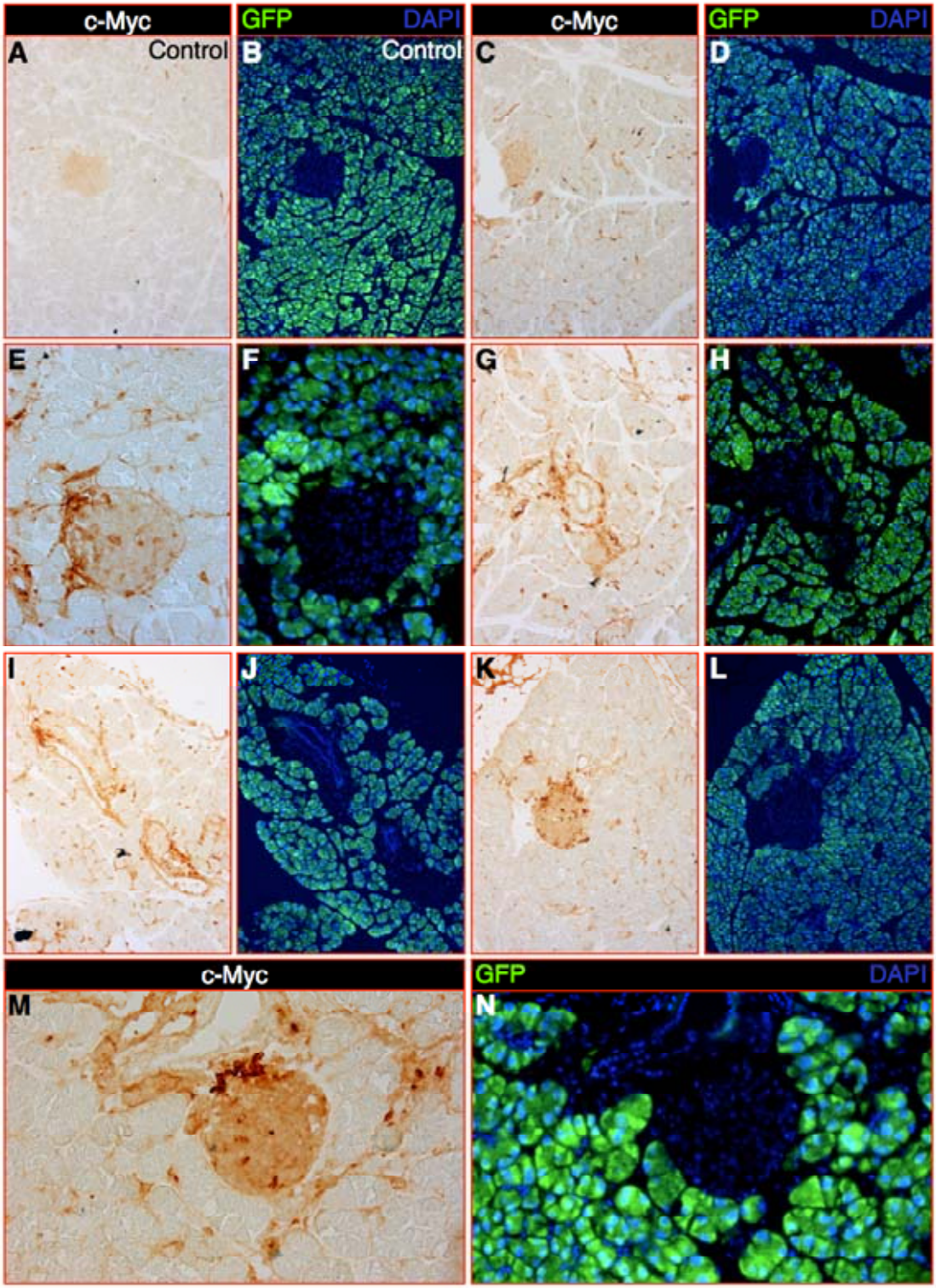

Collombat et al., 2009 - Figure S14

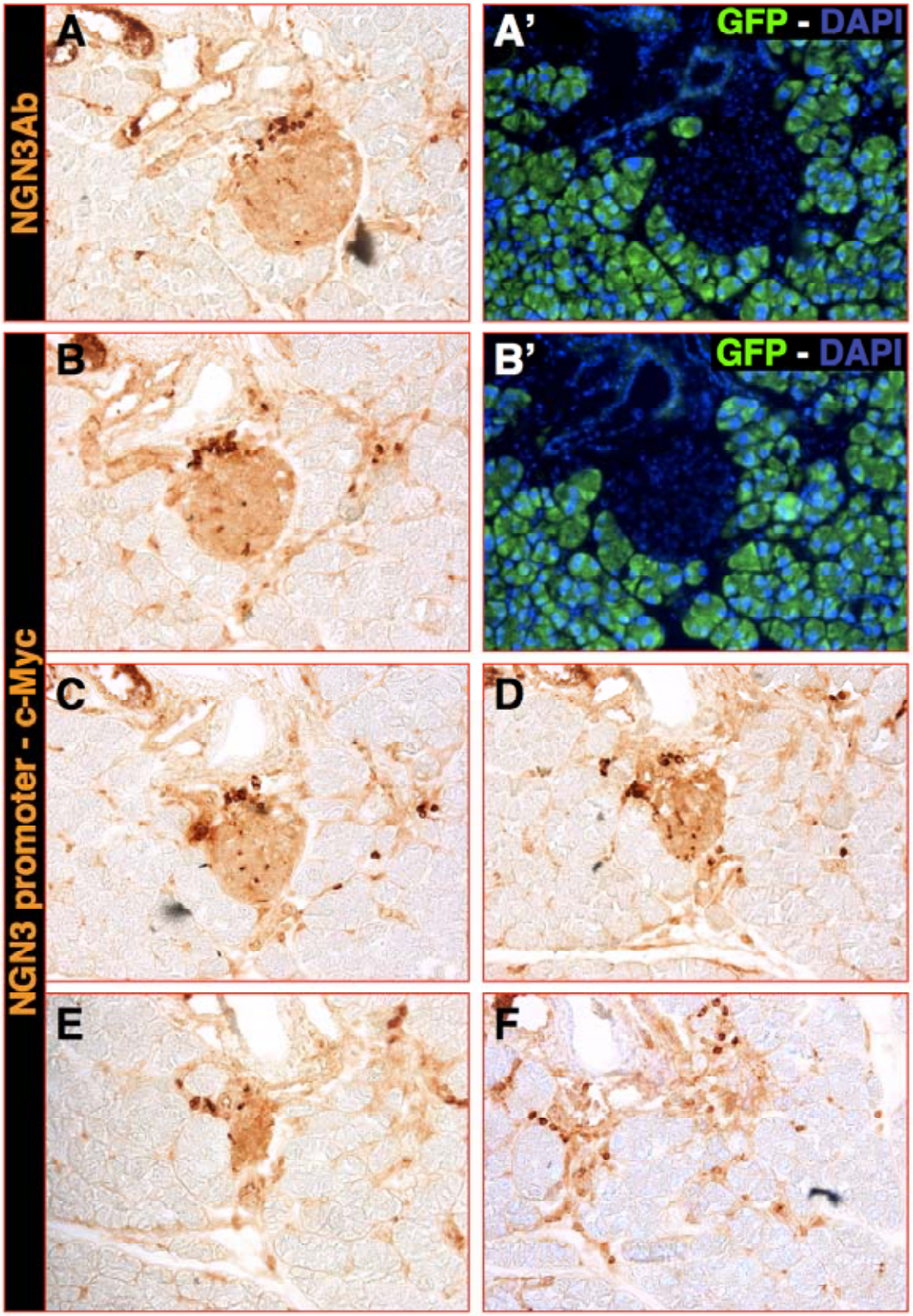

Collombat et al., 2009 - Figure S15

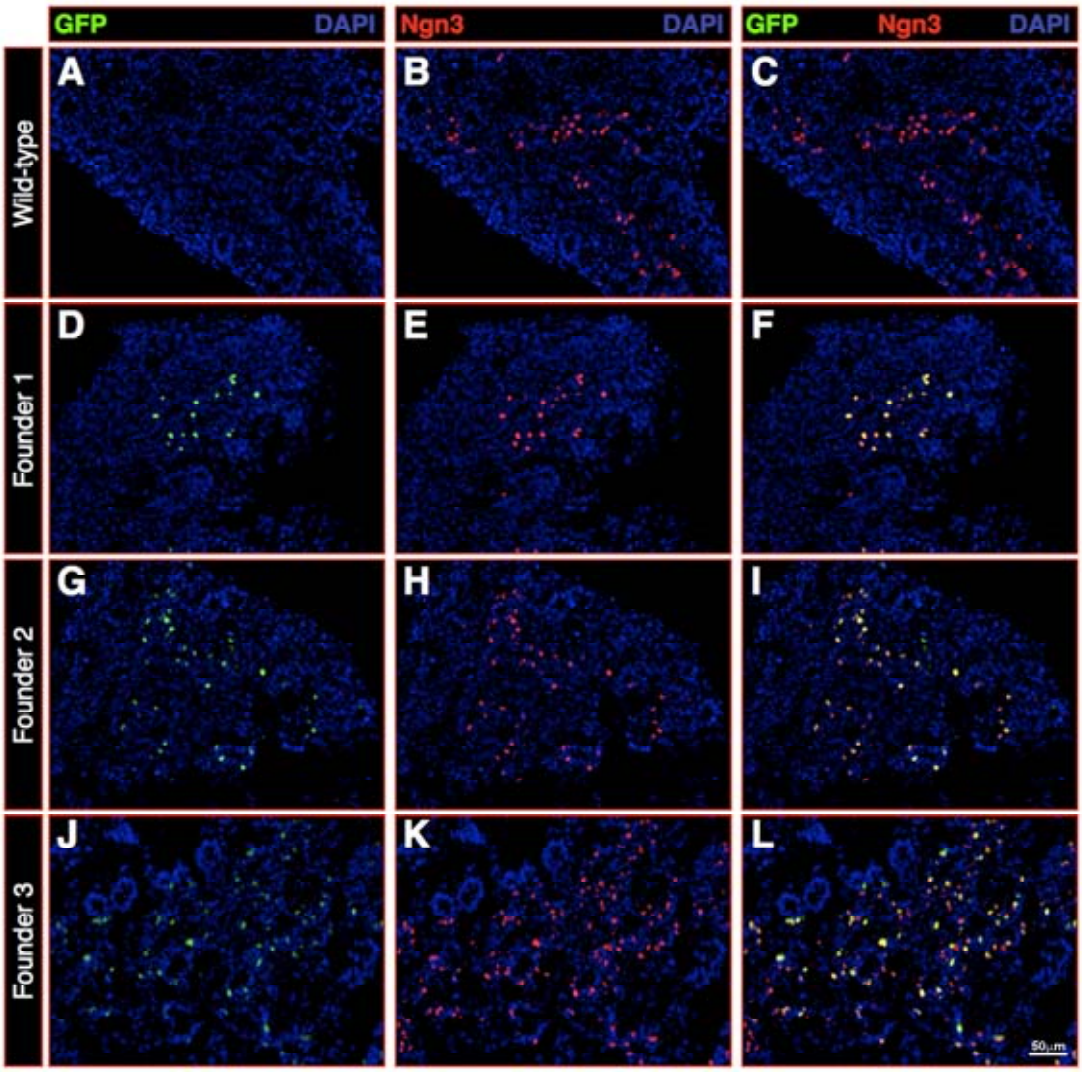

Collombat et al., 2009 - Figure S16

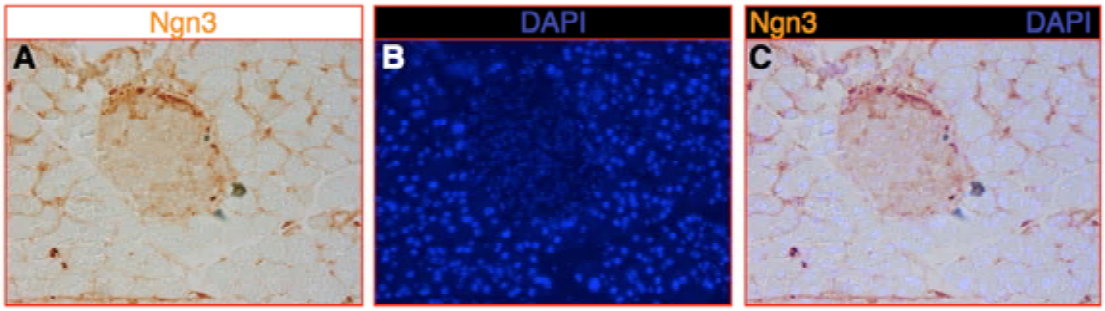

Collombat et al., 2009 - Figure S17

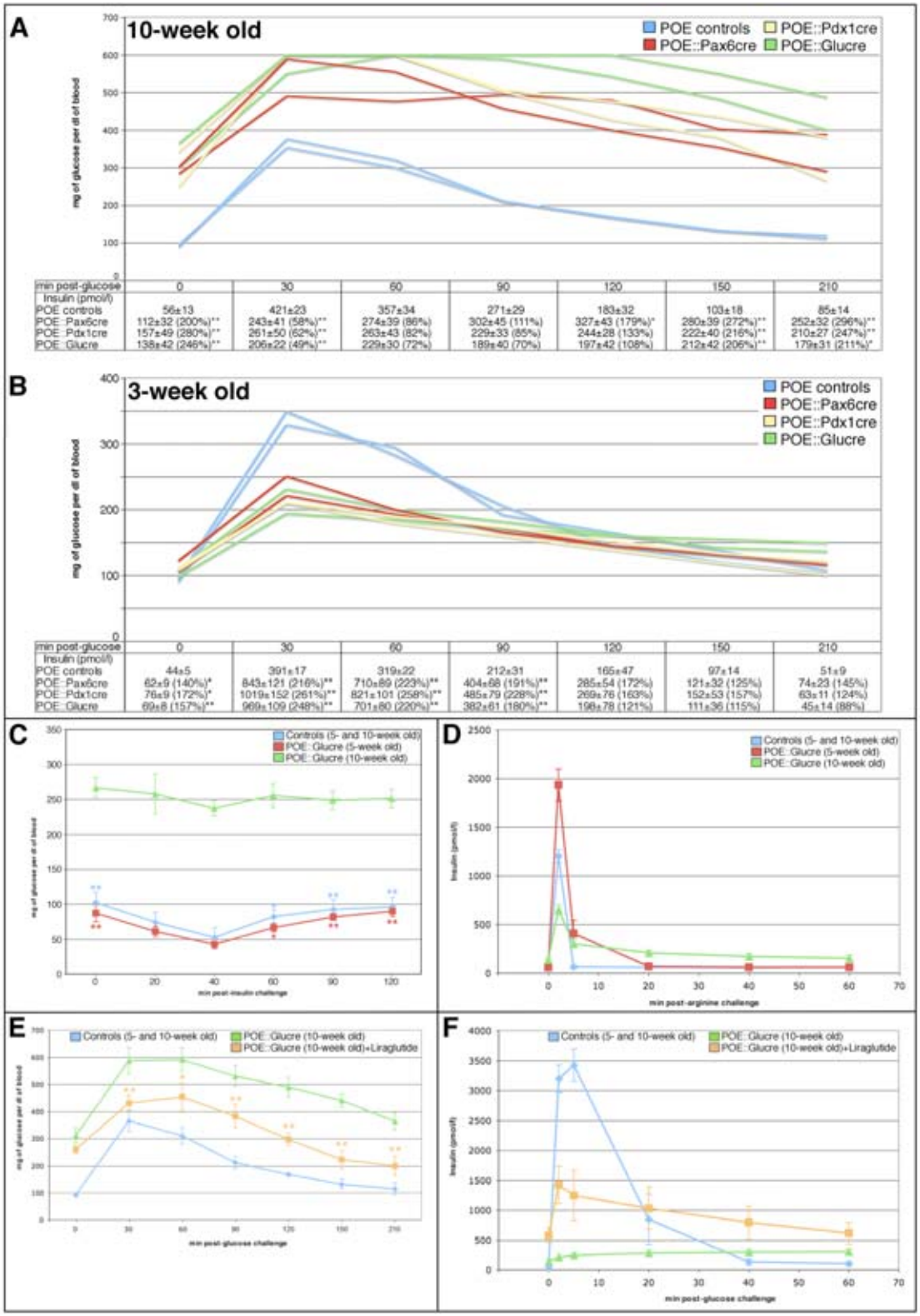

min post-glucose	0	30	60	90	120	150	210
Insulin (pmol/l)							
POE controls	56±13	421±23	357±34	271±29	183±32	103±18	85±14
POE::Pax6cre	112±32 (200%)**	243±41 (58%)**	274±39 (86%)	302±45 (111%)	327±43 (179%)*	280±39 (272%)**	252±32 (296%)**
POE::Pdx1cre	157±49 (280%)**	261±50 (62%)**	263±43 (82%)	229±33 (85%)	244±28 (133%)	222±40 (216%)**	210±27 (247%)**
POE::Glucre	138±42 (246%)**	206±22 (49%)**	229±30 (72%)	189±40 (70%)	197±42 (108%)	212±42 (206%)**	179±31 (211%)*

min post-glucose	0	30	60	90	120	150	210
Insulin (pmol/l)							
POE controls	44±5	391±17	319±22	212±31	165±47	97±14	51±9
POE::Pax6cre	62±9 (140%)*	843±121 (216%)**	710±89 (223%)**	404±68 (191%)**	285±54 (172%)	121±32 (125%)	74±23 (145%)
POE::Pdx1cre	76±9 (172%)*	1019±152 (261%)**	821±101 (258%)**	485±79 (228%)**	269±76 (163%)	152±53 (157%)	63±11 (124%)
POE::Glucre	69±8 (157%)**	969±109 (248%)**	701±80 (220%)**	382±61 (180%)**	196±78 (121%)	111±36 (115%)	45±14 (88%)